PHYSICAL REVIEW A **91**, 010501(R) (2015)

# Measured atomic ground-state polarizabilities of 35 metallic elements

Lei Ma,[1] John Indergaard,[1] Baiqian Zhang,[1] Ilia Larkin,[1] Ramiro Moro,[2] and Walt A. de Heer[1,3,*]

[1]*School of Physics, Georgia Institute of Technology, Atlanta, Georgia 30332, USA*

[2]*Cameron University, Lawton, Oklahoma 73505, USA*

[3]*Department of Physics, KAU, Jeddah 21589, Saudi Arabia*

(Received 29 August 2014; published 7 January 2015)

Advanced pulsed cryogenic molecular-beam electric deflection methods involving position-sensitive mass spectrometry and 7.87-eV ionizing radiation were used to measure the polarizabilities of more than half of the metallic elements in the Periodic Table. Concurrent Stern-Gerlach deflection measurements verified the ground-state condition of the measured atoms. Comparison with state-of-the-art calculations exposes significant systematic and isolated discrepancies throughout the Periodic Table.

DOI: 10.1103/PhysRevA.91.010501 PACS number(s): 32.10.Dk

Static dipole polarizability is a fundamental ground-state property of atoms that has been measured for a few atoms with high precision (see, for example, [1–3]). Despite its relevance, the polarizabilities of less than 1/4 of the elements in the Periodic Table have ever been measured. Not only are atomic polarizabilities important for a variety of applications [4–12], but they also continue to serve as tests for many-body computational methods, which are particularly challenging for atoms with many valence electrons. However, due to the lack of experimental data, often comparisons can only be made with other calculations [13–17]. Here we present the polarizabilities of Na*, Mg, Al*, Sc, Ti, V, Cr, Cu, Ga, Y, Zr, Nb, Mo, Rh, Ag, In*, Sn*, La, Ce, Pr, Nd, Sm, Eu, Gd, Tb, Dy, Ho, Er, Tm, Yb, Lu, Hf, Ta, Pb*, and Bi (an asterisk indicates prior measurement). We show that even when distinct theoretical methods mutually agree [18], surprisingly, in some cases, they disagree with experiment by more than 30%. Rhodium is an extreme case, where the measured polarizability is at least a factor of 2 smaller than the calculated one.

Earlier measurements relied on techniques that required intense and stable molecular beams. For example, in the *E*-*H* balance method the beam passes through an inhomogeneous electric field and an inhomogeneous magnetic field. The fields are adjusted so that the deflections compensate to provide a relationship between the magnetic and induced electric dipole moment [19,20]. The method does not require a measurement of the speed of the atoms, but it does require ground-state paramagnetic atoms with known magnetic moments. Polarizability measurements using the interference of two atomic beams originating from a single source [3,21] are accurate (better than 1%), but the method is not universally applicable.

Metal atoms are particularly challenging, since most have several very low-lying excited states that are typically excited when using standard molecular-beam methods. (For example, Al has an excited state at 112 $cm^{-1}$, V at 137 $cm^{-1}$, Nb at 154 $cm^{-1}$, Sc at 168 $cm^{-1}$, Ti at 170 $cm^{-1}$, Gd at 215 $cm^{-1}$, Ce at 229 $cm^{-1}$, etc. [22].) Consequently, the measurements will not reliably reflect the ground-state polarizabilities. These challenges explain why the atomic polarizabilities of so few elements, and metals in particular, have been measured [18,23].

The molecular-beam apparatus used in the measurements presented here overcomes the experimental obstacles above, allowing accurate polarizability measurements to be performed on the ground state of any stable atom. In principle, this method requires neither intense nor stable beams. The technique is limited essentially only by the photon energy of the laser used to ionize the atoms, as explained next.

The apparatus is schematically shown in Fig. 1. Briefly (for details see Ref. [24]), atoms are produced in a laser vaporization source where pulsed light from a Nd:YAG laser (532 nm, 8-ns pulse width, less than 4 mJ/pulse, 10 Hz) is focused on a metal target in the cryogenically cooled source (whose temperature can be adjusted from $T = 10$ to 300 K), vaporizing a minute amount of metal, on the order of $10^{-3}$ $cm^3/h$ (the target rods were produced from metals obtained from Alfa Aesar with a purity of 99.95% or better). The metal vapor cloud is entrained in a pulse of cryogenically cooled He injected in the source, which cools the vapor, to produce a mixture of atoms and clusters that emerge from a 0.5-mm-diam nozzle. The source parameters are optimized for each material. The resulting beam is collimated using a series of slits and negotiates an inhomogeneous electric field produced by electrodes in the standard two-wire-field geometry [25,26], which is activated to a voltage $V \leqslant 20$ kV, to produce electric fields $E \leqslant 85$ kV/cm, $dE/dz \leqslant 218$ kV/$cm^2$. The deflected beam ultimately enters the position-sensitive time-of-flight (TOF) mass spectrometer, where a pulse of ionizing radiation supplied by an $F_2$ excimer laser (157 nm, 7.89 eV) ionizes a fraction of the atoms (and clusters, when present). A pulsed electric field accelerates the ions towards the ion detector and the arrival times of the ions are digitally recorded using a multichannel scalar with 500-ps channel bin widths. The electric fields in the TOF are adjusted so that the resulting peaks in the TOF spectrum reveal the position of all of the ions in the beam at the time of ionization [see Figs. 2(a) and 2(b)]. When the deflection field is activated, the deflections are manifested as an essentially rigid shift of the beam (with respect to the field-off condition) by a distance $d$ in the direction of the deflecting electric-field gradient. This shift is accurately measured by interleaving field-on and field-off measurements [Figs. 2(a) and 2(b)]. Standard data analysis allows the deflections to be evaluated with a typical accuracy of 10 μm. This accuracy is ultimately determined only by counting statistics, and not by the beam

*walt.deheer@physics.gatech.edu

 

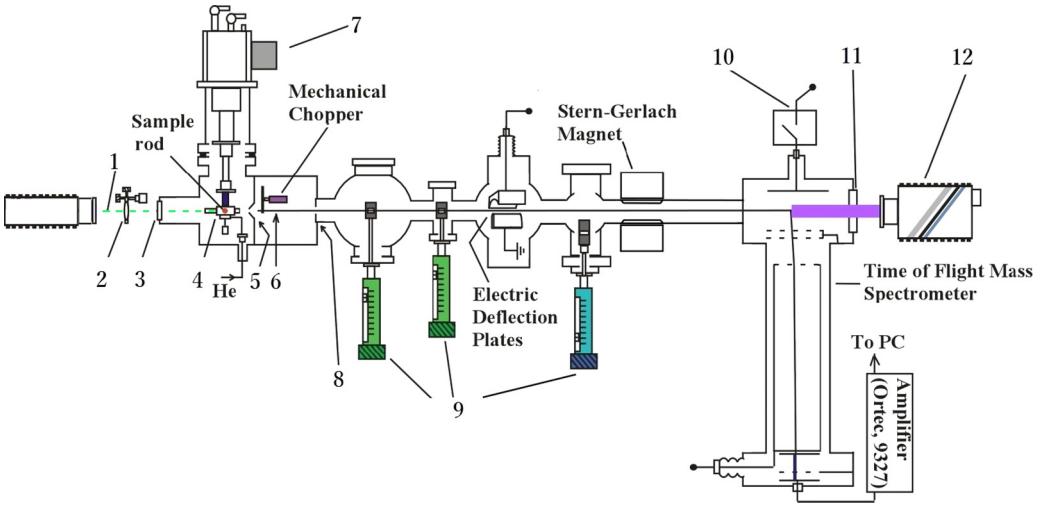


FIG. 1. (Color online) Cryogenic molecular-beam apparatus with position-sensitive time-of-flight mass spectrometer for electric and magnetic deflection measurements (to scale, the source to TOF distance is 2.5 m): 1, YAG laser (Continuum, Surelite I-20, second and third harmonic); 2, lens; 3, window; 4, cryogenic laser vaporization source with cryogenic pulsed valve; 5, skimmer; 6, He carried beam; 7, cryogenic system (Sumitomo SRDK); 8, precollimator; 9, collimators with micrometer activation; 10, ultrafast high-voltage switch (Behlke HTS31); 11, $MgF_2$ window; and 12, $F_2$ excimer laser (GAM EX5).

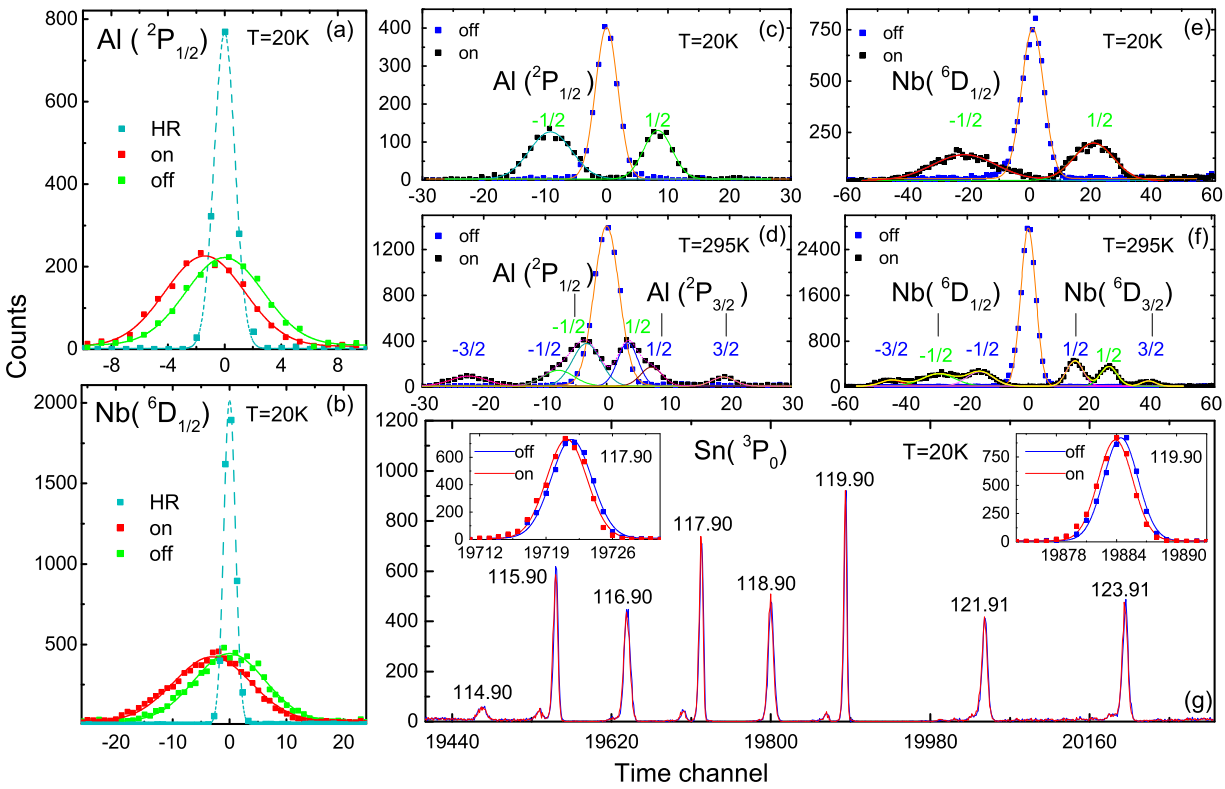


FIG. 2. (Color online) Examples of atomic-beam time-of-flight profiles of several elements; raw data are presented as counts in the indicated time channel [channel 0 is defined to correspond to the beam center of the field off peak for (a)–(f)]. Fits are shown as solid lines. In (a) and (b) high-resolution (HR) (position-insensitive) peaks are shown in blue (dashed gray line), while position-sensitive peaks with the field off are shown in green (solid gray line) and with the field on are shown in red (black line). (a) Electric deflections of ground-state Al at source temperature $T = 20$ K; (b) electric deflections of Nb at $T = 20$ K; (c) Stern-Gerlach deflections of Al at $T = 20$ K corresponding to the $^2P_{1/2}$ ground state; (d) Stern-Gerlach deflections of Al at $T = 295$ K, with an admixture of the $^2P_{3/2}$ excited state ($E = 112$ cm$^{-1}$) observed; (e) Stern-Gerlach deflections of Nb at $T = 20$ K, showing the $^6D_{1/2}$ ground state, (f) at $T = 295$ K revealing an admixture of $^6D_{3/2}$ ($E = 154$ cm$^{-1}$); and (g) position-sensitive time-of-flight mass spectrum of Sn, showing the electric deflections of eight of its stable isotopes indicated by their atomic masses (in atomic units); spurious additional peaks are from the residual gas in the detector.

TABLE I. Comprehensive table containing atomic number, electronic configuration (Config.), term symbol, and our measured polarizability (Pol.) and uncertainty (Unc.) for each element studied in this work. The uncertainties shown here do not include the contribution from the Al calibration.

| Element | | Config. | Term | Pol. (Å$^3$) | Unc. (Å$^3$) | Element | | Config. | Term | Pol. (Å$^3$) | Unc. (Å$^3$) |
|---|---|---|---|---|---|---|---|---|---|---|---|
| 11 | Na | $3s^1$ | $^2S_{1/2}$ | 23.8 | 1.1 | 58 | Ce | $4f^15d^16s^2$ | $^1G^\circ_4$ | 28.4 | 3.0 |
| 12 | Mg | $3s^2$ | $^1S_0$ | 8.8 | 2.3 | 59 | Pr | $4f^36s^2$ | $^4I^\circ$ | 35.4 | 4.1 |
| 13 | Al | $3s^24s^1$ | $^2P^\circ_{1/2}$ | 6.8 | 0.3 | 60 | Nd | $4f^46s^2$ | $^5I_4$ | 27.2 | 2.9 |
| 21 | Sc | $3d^14s^2$ | $^2D_{3/2}$ | 14.4 | 1.4 | 62 | Sm | $4f^66s^2$ | $^7F_0$ | 23.2 | 2.4 |
| 22 | Ti | $3d^24s^2$ | $a\,^3F_2$ | 9.4 | 0.5 | 63 | Eu | $4f^76s^2$ | $a\,^8S^\circ_{7/2}$ | 21.6 | 3.7 |
| 23 | V | $3d^34s^2$ | $a\,^4F_{3/2}$ | 10.1 | 0.8 | 64 | Gd | $4f^75d^16s^2$ | $^9D^\circ_2$ | 26.1 | 3.9 |
| 24 | Cr | $3d^54s^1$ | $a\,^7S_3$ | 8.9 | 3.5 | 65 | Tb | $4f^96s^2$ | $^6H^\circ_{15/2}$ | 23.5 | 1.6 |
| 29 | Cu | $3d^{10}4s^1$ | $^2S_{1/2}$ | 8.7 | 0.7 | 66 | Dy | $4f^{10}6s^2$ | $^5I_8$ | 23.3 | 1.6 |
| 31 | Ga | $4s^24p^1$ | $^2P^\circ_{1/2}$ | 6.9 | 0.6 | 67 | Ho | $4f^{11}6s^2$ | $^4I^\circ_{15/2}$ | 21.5 | 1.7 |
| 39 | Y | $4d^15s^2$ | $^2D_{3/2}$ | 24.1 | 1.7 | 68 | Er | $4f^{12}6s^2$ | $^3H_6$ | 32.2 | 5.7 |
| 40 | Zr | $4d^25s^2$ | $a\,^3F_2$ | 16.6 | 1.9 | 69 | Tm | $4f^{13}6s^2$ | $^2F^\circ_{7/2}$ | 19.2 | 2.4 |
| 41 | Nb | $4d^45s^1$ | $a\,^6D_{1/2}$ | 14.5 | 1.1 | 70 | Yb | $4f^{14}6s^2$ | $^1S_0$ | 21.8 | 2.9 |
| 42 | Mo | $4d^55s^1$ | $a\,^7S_3$ | 12.9 | 0.9 | 71 | Lu | $5d^16s^2$ | $^2D_{3/2}$ | 18.3 | 2.7 |
| 45 | Rh | $4d^85s^1$ | $a\,^4F_{9/2}$ | 1.6[a] | −1.6/+3.2[a] | 72 | Hf | $5d^26s^2$ | $^3F_2$ | 12.4 | 2.8 |
| 47 | Ag | $4d^{10}5s^1$ | $^2S_{1/2}$ | 6.8 | 1.1 | 73 | Ta | $5d^36s^2$ | $^4F_{3/2}$ | 8.6 | 1.8 |
| 49 | In | $5p^1$ | $^2P^\circ_{1/2}$ | 9.2 | 0.9 | 82 | Pb | $6p^2{}_{1/2}$ | (1/2,1/2) | 8.3 | 2.7 |
| 50 | Sn | $5p^2$ | $^3P_0$ | 10.0 | 1.3 | 83 | Bi | $6p^3$ | $^4S^\circ_{3/2}$ | 8.1 | 1.7 |
| 57 | La | $5d^16s^2$ | $^2D_{3/2}$ | 25.3 | 1.2 | | | | | | |

[a]The polarizability for Rh is anomalously low.

width, beam stability, nor temporal separation of the channels in the multichannel scalar. (For details of the data analysis, see Refs. [27–30].) When the TOF fields are adjusted for the high-resolution mass spectrometry mode, the peaks do not shift and the TOF has a mass resolution $m/\Delta m = 10^4$ (in the position-sensitive mode $m/\Delta m = 10^3$), as shown in Figs. 2(a) and 2(b). The parameters in the TOF can be instantaneously switched from the position-insensitive high-resolution mass spectroscopy mode (also known as the spatial focusing mode) to the position-sensitive mass spectroscopy mode. Such high resolution allows us to simultaneously measure the electric deflections of elements with several isotopes, as shown in Fig. 2(g) in the case of Sn.

A chopper just downstream of the source passes a small pulse of atoms in each cycle (for details, see Refs. [24,31]). The ionization laser is synchronized with the chopper. The velocity of the selected atoms is evaluated with typically 0.5% accuracy. The polarizability $\alpha$ is found from

$$d = \alpha E \frac{\partial E}{\partial z}\left(L + \frac{l}{2}\right)\frac{l}{mv^2} = K\alpha\frac{V^2}{mv^2}, \qquad (1)$$

where $E$ is the electric field (proportional to the applied voltage $V$), $\partial E/\partial z$ is the field gradient in the inhomogeneous electric field, $L$ is the distance from the field to the detector, and $l$ is the length of the deflecting field; $K$ lumps these constants together. Since Al reliably produces intense atomic beams, we used Al as our standard reference. Calibration runs using Al were performed in the course of each measurement. The quality of Al calibration (measured to be $\alpha_{\rm Al} = 6.8 \pm 0.3$ Å$^3$ in [24]) can be judged based on the comparison between our measured value of $\alpha_{\rm Na} = 23.8 \pm 1.1$ Å$^3$ for sodium and ultrahigh-precision measurement made in Ref. [3]. Note that the same apparatus was used for metal cluster polarizability measurements [32,33], for which the polarizabilities are found to accurately converge to their bulk metal limits (i.e., $\alpha_{\rm bulk} = R^3_{\rm bulk}$, where $R_{\rm bulk}$ is the bulk atomic radius [34]).

The molecular-beam apparatus is also supplied with a Stern-Gerlach magnet (see Fig. 1). The number of peaks in the magnetic deflections [see Figs. 2(c)–2(f)] of a specific atom corresponds to $2J + 1$, where $J$ is the atomic angular momentum quantum number, whose value is known for all ground states and excited states of the atoms measured. We have verified that the atoms were indeed in their ground states (note that we were also able to produce beams at higher temperatures that contained excited state atoms [Figs. 2(e) and 2(f)], but no attempts were made to measure excited-state polarizabilities). The atomic-beam temperature is determined from the relative population of the excited states to ground states using Boltzmann statistics, revealing that it closely follows the source temperature [26]. This indicates that the source effectively cools the atoms. It is particularly important for atoms that have excited states that are excited even below room temperature (i.e., Al, Sc, Ti, V, and Nb), requiring the efficient cryogenic cooling provided by our source.

Results of the measurements are reported in Table I and plotted in Fig. 3, which also presents theoretical results. The well-known shell structure trend, where the polarizability is the greatest at the opening of an atomic shell (i.e., at the alkali-metal atoms) and progressively diminishes at the closing of the shell (i.e., at the inert gases), is clearly observed. Our measurements agree with measurements of five elements (Na, Al, In, Sn, and Pb) that were previously measured. However, significant discrepancies are observed for theoretical predictions of specific atoms as well as in trends. For example, $\alpha_{\rm Al}$ is measured to be 20% smaller than several calculations and $\alpha_{\rm Mg}$ is also smaller than the predicted value. For the $4d$ transition metals, the local-density approximation

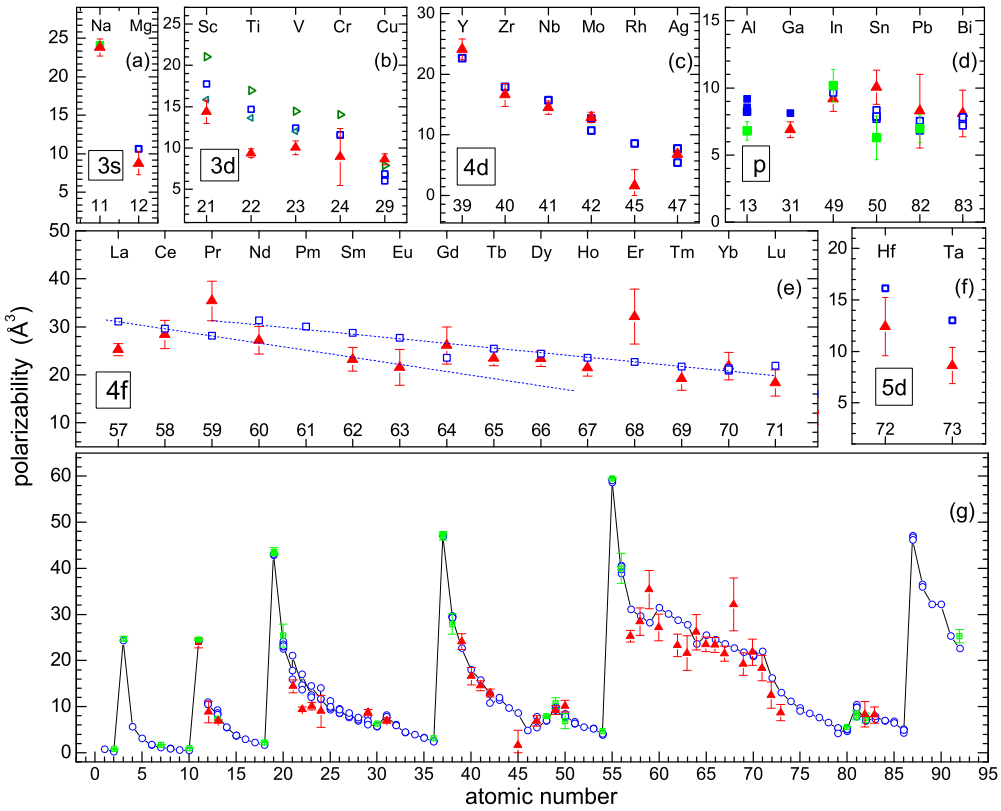


FIG. 3. (Color online) Overview of atomic polarizabilities: (a)–(f) measured and calculated polarizabilities organized by atomic orbital type $s$, $p$, $d$, and $f$ and (g) calculated values (open blue circles, from Ref. [18] and references therein), previously measured values (green squares, from Refs. [3,21,28,35]), measured values in this work (red triangles).

(LDA) predictions agree with the experimental values, but it significantly overestimates the polarizabilities for the $3d$ and $5d$ metals. The variational perturbation approach appears to be more accurate for the $3d$ metals, but still large discrepancies (greater than 30% for Ti) are observed [18]. For Cu, experiment and theory agree well. On the other hand, for $_{45}$Rh ($4d^8 5s^1$) the measured polarizability is 1.6 Å$^3$ (comparable to $_{36}$Kr), while the predicted value is 8.57 Å$^3$, representing the largest discrepancy that we have measured. The LDA predictions for the lanthanides ($4f$) are reasonably accurate, however, nonsystematic discrepancies (both positive and negative) on the order of 20% are observed. Polarizabilities of the $p$-block metals [Fig. 3(d)] show significant discrepancies for Al and Ga, but In, Sn, Pb, and Bi are all in reasonable agreement with various theories.

In conclusion, despite their importance for atomic physics and computational physics, atomic polarizabilities of relatively few atoms had been measured. Here we have presented the ground-state polarizabilities of half of the (stable) metallic elements in the Periodic Table. Experiment and theory agree well in about half of the cases. Several significant systematic discrepancies (e.g., in the $3d$ metals) and several isolated large discrepancies (i.e., Al and Rh) compared with theory were noted. Since various theoretical approaches tend to agree with each other better than with experiment, it suggests that our measurements may have uncovered systematic theoretical problems and therefore may help future developments in many-body theory. The accuracy of the measurements provided here can be significantly improved with further developments of the technique. These polarizability measurements will be extended to dimers, many of which have been calculated, but not measured.

The National Science Foundation is gratefully acknowledged for financial support under Grant No. DMR1308835.

[1] J. W. Schmidt, R. M. Gavioso, E. F. May, and M. R. Moldover, Phys. Rev. Lett. **98**, 254504 (2007).

[2] J. M. Amini and H. Gould, Phys. Rev. Lett. **91**, 153001 (2003).

[3] C. R. Ekstrom, J. Schmiedmayer, M. S. Chapman, T. D. Hammond, and D. E. Pritchard, Phys. Rev. A **51**, 3883 (1995).

[4] G. Maroulis and C. Pouchan, J. Phys. B **36**, 2011 (2003).

[5] J. Mitroy, M. S. Safronova, and C. W. Clark, J. Phys. B **43**, 202001 (2010).

[6] M. T. Murphy, J. K. Webb, and V. V. Flambaum, Phys. Rev. Lett. **99**, 239001 (2007).

[7] T. Rosenband, D. B. Hume, P. O. Schmidt *et al.*, Science **319**, 1808 (2008).

[8] T. F. Gallagher and W. E. Cooke, Phys. Rev. Lett. **42**, 835 (1979).

[9] W. M. Itano, L. L. Lewis, and D. J. Wineland, Phys. Rev. A **25**, 1233 (1982).
[10] S. G. Porsev and A. Derevianko, Phys. Rev. A **74**, 020502 (2006).
[11] A. D. Ludlow *et al.*, Science **319**, 1805 (2008).
[12] J. A. Sherman, N. D. Lemke, N. Hinkley, M. Pizzocaro, R. W. Fox, A. D. Ludlow, and C. W. Oates, Phys. Rev. Lett. **108**, 153002 (2012).
[13] M. S. Safronova and W. R. Johnson, Adv. At. Mol. Opt. Phys. **55**, 191 (2008).
[14] B. Arora, M. S. Safronova, and C. W. Clark, Phys. Rev. A **76**, 052509 (2007).
[15] A. Derevianko, W. R. Johnson, M. S. Safronova, and J. F. Babb, Phys. Rev. Lett. **82**, 3589 (1999).
[16] A. Hibbert, Rep. Prog. Phys. **38**, 1217 (1975).
[17] V. A. Dzuba, V. V. Flambaum, and M. G. Kozlov, Phys. Rev. A **54**, 3948 (1996).
[18] P. Schwerdtfeger, Table of Experimental and Calculated Static Dipole Polarizabilities for the Electronic Ground States of the Neutral Elements (Centre for Theoretical Chemistry and Physics, Albany, 2014), and references therein, http://ctcp.massey.ac.nz/index.php?menu=dipole&page=dipole
[19] R. W. Molof, H. L. Schwartz, T. M. Miller, and B. Benderson, Phys. Rev. A **10**, 1131 (1974).
[20] H. L. Schwartz, T. M. Miller, and B. Bederson, Phys. Rev. A **10**, 1924 (1974).
[21] W. F. Holmgren, M. C. Revelle, V. P. A. Lonij, and A. D. Cronin, Phys. Rev. A **81**, 053607 (2010).
[22] NIST, Basic Atomic Spectroscopic Data, and references therein, http://physics.nist.gov/PhysRefData/Handbook/periodictable.htm
[23] *CRC Handbook of Chemistry and Physics*, 94th ed. (CRC, Boca Raton, 2013), pp. 10–188, and references therein.
[24] P. Milani, I. Moullet, and W. A. de Heer, Phys. Rev. A **42**, 5150 (1990).
[25] G. Scoles, D. Bassi, U. Buck, and D. C. Laine, *Atomic and Molecular Beam Methods: Volume 1* (Oxford University Press, Oxford, 1988).
[26] See Supplemental Material at http://link.aps.org/supplemental/10.1103/PhysRevA.91.010501 for beam deflection profiles of measured elements; additional ground state confirmation results for Sn and Ti; Beam temperature measurement based on aluminum deflection experiments; Geometric structure of deflection electrodes.
[27] M. K. Beyer and M. B. Knickelbein, J. Chem. Phys. **126**, 104301 (2007).
[28] C. Thierfelder, B. Assadollahzadeh, P. Schwerdtfeger, S. Schäfer, and R. Schäfer, Phys. Rev. A **78**, 052506 (2008).
[29] S. Schäfer, M. Mehring, R. Schäfer, and P. Schwerdtfeger, Phys. Rev. A **76**, 052515 (2007).
[30] C. Lupinetti and A. J. Thakkar, J. Chem. Phys. **122**, 044301 (2005).
[31] W. A. de Heer and P. Milani, Rev. Sci. Instrum. **62**, 670 (1991).
[32] J. Bowlan, A. Liang, and W. A. de Heer, Phys. Rev. Lett. **106**, 043401 (2011).
[33] R. Moro, X. Xu, S. Yin, and W. A. de Heer, Science **300**, 1265 (2003).
[34] C. Kittel, *Introduction to Solid State Physics*, 7th ed. (Wiley, New York, 1996), p. 412.
[35] T. P. Guella, T. M. Miller, B. Bederson, J. A. D. Stockdale, and B. Jaduszliwer, Phys. Rev. A **29**, 2977 (1984).